Role of iron in the incorporation of uranium in ferric garnet matrices

Zs. Rák,* R. C. Ewing, and U. Becker
Department of Geological Sciences, University of Michigan, Ann Arbor, Michigan 48109, USA
(Received 30 June 2011; published 18 October 2011)

The structural relaxations and electronic structure of U-containing $Ca_3(Ti,Zr,Hf,Sn)_2(Fe_2Si)O_{12}$ garnet systems have been investigated using *ab initio* methods within density functional theory (DFT) in the generalized gradient approximation with a Hubbard correction U (GGA + U). The calculations provide a fundamental understanding of the role of Fe in the incorporation and stability of U in the garnet structure. The atomic relaxations around U are controlled by a delicate balance between the Coulomb interactions among the ions and the size effect of the large U atom. The relaxation pattern indicates that when U occupies the *A* site, a charge transfer occurs from U to its nearest-neighbor (NN) Fe atom. This is further verified by the detailed analysis of the electronic band structures and charge density distribution. The double exchange coupling of the U *f* and the NN Fe *d* shells via the transfer of electrons lowers the energy of the system when the spins of the *f* and *d* shells are antiparallel. The incorporation energy of U at the *A* site (substituting Ca) increases dramatically with the decrease in the number of Fe atoms in the neighboring tetrahedral sites. The presence of Fe is crucial, since it accommodates the extra valence electrons introduced by U and the electron transfer allows the lowering of the total energy of the structure. Comparing the incorporation energies at the *A* and *B* site (octahedral site), U clearly prefers the A site, provided that there are sufficient Fe atoms in its vicinity to facilitate the charge transfer.

DOI: 10.1103/PhysRevB.84.155128 PACS number(s): 71.15.Mb, 71.20.Ps, 71.55.Ht

I. INTRODUCTION

A continuing concern with the potential expansion in nuclear power generation is the safe disposal and isolation of both the spent fuel from nuclear reactors and the high-level wastes (HLW) generated mainly by reprocessing the spent nuclear fuel. In order to dispose of highly-radioactive or long-lived radionuclides (half-life: $^{239}Pu = 24{,}100$ years, $^{237}Np = 2.1$ million years), there has been an increased interest in designing and developing specific materials for actinide incorporation, which would allow the radioactivity to decay while the materials retain their integrity for hundreds of thousands of years.[1–3] A recently investigated structure is garnet.[4] Numerous studies have been completed on a wide range of compositions with the garnet structure, specifically on its capacity to incorporate actinides,[5,6] radiation resistance,[7–11] and stability in aqueous solutions.[5,9,12]

Garnet, $A_3B_2X_3O_{12}$ (*Ia3d*, $Z = 8$), is a common mineral in nature with a wide variety of compositions because it has three cation sites: *A* site (8-coordinated, dodecahedral), *B* site (6-coordinated, octahedral), and *X* site (4-coordinated, tetrahedral). Most natural garnets are silicates, with Si^{4+} occupying the tetrahedral site (*X* site). In spite of the compositional diversity, the actinide content in natural garnet is very low (usually less than 0.1 %). Nevertheless, it has been found that synthetic ferrites with garnet structure in which the Si^{4+} ions (at the *X* site) are replaced by Fe^{3+}, have a high capacity to incorporate actinides (e.g., up to 30 wt% of U).[5,6] This suggests that the garnet structure is a good candidate for the incorporation of uranium and, possibly, other actinides, such as Pu and Np. The explanation for the increased actinide capacity has been that the structural polyhedra together with unit cell size increase when the small Si atom is replaced by the larger Fe. As a result, the large actinide elements can easily be accommodated in the structure.[13] In addition to this rather simplistic explanation, we find that the coupling between the partially filled *f* and *d* shells of the actinides and Fe, respectively, play a crucial role in the incorporation mechanism of actinides into the garnet structure.

We have described the electronic structure of $Ca_3(Ti, Zr, Hf, Sn)_2(Fe_2Si)O_{12}$ garnet systems and calculated the energies required to incorporate uranium at the *A* and *B* sites of the structure.[14] The motivation for additional investigations was stimulated by the recent discovery of a natural uranian-garnet, elbrusite-(Zr), with a U content as high as 27 wt%.[15] The chemical formula of the end member of elbrusite-(Zr) is $Ca_3(U^{6+}Zr)(Fe_2^{3+}Fe^{2+})O_{12}$, and it has been described to form a complex solid solution with kimzeyite ($Ca_3Zr_2Fe_2^{3+}SiO_{12}$), schorlomite ($Ca_3Ti_2Fe_2^{3+}SiO_{12}$), and toturite ($Ca_3Sn_2Fe_2^{3+}SiO_{12}$). We note that the low silicon concentration (0.6–1.1 wt%) and the high Fe content of this newly discovered uranian garnet is similar to that of synthetic, actinide-bearing ferrigarnets.

In this paper, we further explore the energetics of the $Ca_3(Ti, Zr, Hf, Sn)_2(Fe_2Si)O_{12}$ system by investigating the electronic structure of the U-containing garnet. In order to obtain a fundamental understanding of the incorporation mechanism and the stability of U inside the garnet structure, we have analyzed the details of the electronic interactions between the partially filled U *f*shell and the neighboring Fe *d* shells. In order to clarify the role of Fe, the U incorporation energies (E_{inc}) have been recalculated for several different ionic configurations for which the number of Fe atoms in the vicinity of U is varied.

The incorporation of U at the *A* site of the garnet structure can be regarded in two, slightly different ways. In the first case, from the viewpoint of semiconductor physics, since the neutral U ($5f^36d^17s^2$) atom has more electrons outside a closed shell than the neutral Ca atom ($4s^2$), it can be regarded as a donor impurity, which provides extra electrons to the system. When U substitutes a Ca atom, two of the valence electrons of the U atom will form bonds with its neighbors (the same way the two electrons of Ca did), while the remaining valence

electrons (1, 2, 3, or 4, depending on the oxidation state of U) are "donated" to the conduction band (CB). In the second case, the incorporation of U^{4+} (U^{3+}) ion at the *A* site can be regarded as a coupled substitution in which one Ca^{2+} and two (one) Fe^{3+} ions are replaced by U^{4+} (U^{3+}) and two (one) Fe^{2+}ions.

In the first part of the paper, when we discuss the electronic structure of the U-containing systems, we adopt the band-theoretical point of view in which the extra valence electrons introduced by U are transferred and become localized on the neighboring Fe atoms. In the second part of the paper, where we calculate the incorporation energies of U, we make use of the coupled substitution scheme in order to describe the reaction paths by which U is introduced into the garnet matrix.

II. METHODS

The calculations have been performed using the projector augmented wave (PAW)[16,17] method within density functional theory (DFT)[18,19] as implemented in the Vienna *ab initio* simulation package (VASP).[20–23] The exchange-correlation potential was approximated by the generalized gradient approximation (GGA), as parameterized by Perdew, Burke, and Ernzerhof (PBE).[24] The cutoff energy for the plane-wave basis was set to 450 eV, and the convergence of self-consistent cycles was assumed when the energy difference between them was less than 10^{-5} eV. The standard PAW potentials provided with the VASP code were used in the calculations.

In order to describe the behavior of the localized Fe *d* and U *f* states, we have included the orbital-dependent, on-site Coulomb potential (Hubbard *U*) and the exchange parameter *J* in the calculations within the GGA+*U* method.[25,26] The values of the Hubbard *U* parameter can be estimated from band-structure calculations in the supercell approximation with different *d* and *f* occupations.[27] Here, we treat *U* and *J* as adjustable parameters using the following values: $U(\mathrm{Fe}_d) = 4.8$ eV with the corresponding $J(\mathrm{Fe}_d) = 0.5$ eV, respectively, and $U(\mathrm{U}_f) = 4.5$ eV with $J(\mathrm{U}_f) = 0.5$ eV. These are physically reasonable values, which have been previously used in the literature.[14,25,28,29]

The effect of the Hubbard *U* parameter on the electronic structure of $Ca_3B_2(Fe_2Si)O_{12}$, (B = Ti, Zr, Hf, Sn) garnet systems has been investigated earlier[14] for three different values of $U(\mathrm{Fe}_d)$. As the *U* value increases (from $U = 0$ to 4.8 and 6.8 eV) the band gaps become wider, the Fe *d* states become more localized and the Fe magnetic moments are enhanced. Changing the value of $U(\mathrm{Fe}_d)$ would have similar effects on the electronic structure of the U-containing systems. The value of $U(\mathrm{U}_f)$ influences the energies and degree of localization of the U *f* orbitals and consequently the electronic structure of the U-containing systems would be slightly different (the position of the empty U *f* orbitals in the CB, as described in Sec. III C, would shift up or down, depending on the $U(\mathrm{U}_f)$ value. Nevertheless, since the calculations have to be carried out using the same values of $U(\mathrm{U}_f)$ for all U-containing systems (including UO_2), the calculated incorporation energies and the observed trends are most likely correct.

The results described in the present paper have been obtained using the previously calculated lattice constants.[14] The ionic relaxations have been completed with the same parameters as described in Ref. 14, but here we have used a slightly different method: while in Ref. 14, the relaxations were performed without the inclusion of the Hubbard *U*parameters, here we have included them in the calculations. As a result, the E_{inc} presented in this paper are somewhat different from those in Ref. 14. In addition, the incorporation energies were also calculated as a function of the number of Fe atoms located in the vicinity of the U, for the two possible spin orientations of the incomplete U *f* shell.

In the case of heavy elements, such as uranium, the inclusion of relativistic effects is quite significant. However, due to the considerable computational power required to perform fully relativistic calculations on a large system (160 atoms/unit cell), we have carried out the calculations at the scalar relativistic level. In this approximation, the relativistic effects due to the Darwin and mass-velocity terms are taken into account, and the spin-orbit (SO) interaction is neglected. Since the SO splitting in the U 5*f* shell is of the order of 1–2 eV,[30] neglecting the SO interaction, may also have an influence on the calculated electronic structure of the U-containing garnet systems. However, since the incorporation energies are calculated from total energy differences, we expect that the errors introduced by neglecting the SO interaction have very little effect on results reported in the present work.

III. RESULTS AND DISCUSSIONS

A. Structural relaxations around the uranium site

1. Uranium at the A site

In Fig. 1(a), we show the dodecahedral site (*A* site), coordinated by eight oxygen atoms, each of which is connected to a tetrahedral site (*X* site, which can be occupied by Fe or Si). Four out of the eight O atoms are connected to distinct tetrahedral sites, while the remaining four are shared by two tetrahedra. These two sites, denoted as X_1 and X_2 in Fig. 1(a), are situated closer to the *A* site, as compared with the other neighboring *X* sites. In the garnet structure, with no U atoms, the distance between the *A* and $X_{1,2}$ sites varies

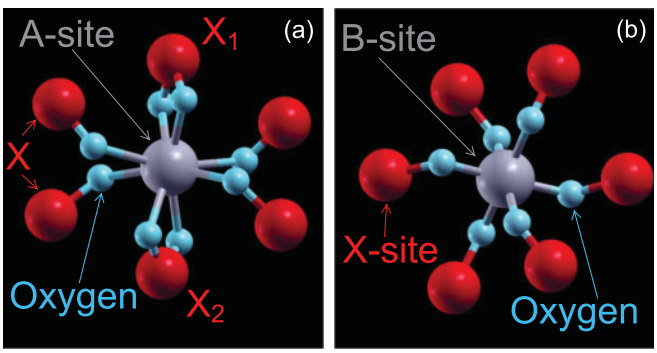

FIG. 1. (Color online) Dodecahedral and octahedral sites (*A* and *B* sites, respectively) of the garnet structure. (a) The *A* site is coordinated by eight O atoms, four of which connect to individual tetrahedral sites (*X* sites), while the remaining four O's are shared by two tetrahedral sites (X_1 and X_2). (b) The octahedral site is sixfold coordinated by O's and each O is connected to a tetrahedral site (*X* site). The tetrahedral sites are occupied by Fe and Si.

TABLE I. The average U-O separations (four O's connected to the X sites, two O's connected to the X_1 site, and two O's connected to X_2 site) as well as the U-$X_{1,2}$ distances. The negative values indicate inward relaxation (toward the U atom), while the positive values indicate outward relaxation (away from the U atom). All distances are given in Å.

		$X_1 = X_2 =$ Fe		$X_1 =$ Fe, $X_2 =$ Si		$X_1 = X_2 =$ Si	
System	bond	distance (Å)	% change	distance (Å)	% change	distance (Å)	% change
$Ca_3Ti_2(Fe_2Si)O_{12}$	U-O (X)	2.50	−1.28%	2.50	−3.16%	2.50	−0.17%
	U-O (X_1)	2.30	−4.60%	2.24	−5.87%	2.47	1.43%
	U-O (X_2)	2.34	−3.62%	2.45	0.54%	2.49	1.24%
	U-X_1	3.18	2.13%	3.15	0.72%	3.15	2.01%
	U-X_2	3.23	2.51%	3.17	3.03%	3.17	1.64%
$Ca_3Zr_2(Fe_2Si)O_{12}$	U-O (X)	2.53	−1.33%	2.53	−3.74%	2.51	−1.09%
	U-O (X_1)	2.29	−6.72%	2.24	−7.01%	2.54	1.32%
	U-O (X_2)	2.34	−4.95%	2.50	0.39%	2.53	1.59%
	U-X_1	3.25	1.38%	3.24	1.35%	3.24	1.63%
	U-X_2	3.29	2.18%	3.24	2.39%	3.22	1.90%
$Ca_3Hf_2(Fe_2Si)O_{12}$	U-O (X)	2.54	−0.99%	2.53	−3.67%	2.51	−1.13%
	U-O (X_1)	2.31	−5.87%	2.23	−6.74%	2.54	1.62%
	U-O (X_2)	2.32	−5.43%	2.50	0.56%	2.53	1.93%
	U-X_1	3.27	2.29%	3.22	1.38%	3.23	1.75%
	U-X_2	3.28	2.36%	3.24	2.55%	3.20	1.96%
$Ca_3Sn_2(Fe_2Si)O_{12}$	U-O (X)	2.54	−0.56%	2.53	−2.87%	2.50	−0.85%
	U-O (X_1)	2.32	−5.52%	2.25	−5.80%	2.52	1.91%
	U-O (X_2)	2.31	−5.38%	2.47	0.44%	2.51	1.51%
	U-X_1	3.28	2.40%	3.22	1.83%	3.22	2.14%
	U-X_2	3.27	2.53%	3.23	2.56%	3.21	1.69%

from approximately 3.1 to 3.2 Å, depending on the atomic species (Si or Fe) occupying the $X_{1,2}$ sites, while the distance between the A site and the four other X sites is around 3.9 Å. We expect that the charge transfer between U, situated at the A site, and Fe will take place with a higher probability if Fe occupies the X_1 and X_2 sites. In order to verify this assumption, we have performed calculations using three different atomic arrangements: (i) both X_1 and X_2 sites occupied by Fe, (ii) X_1 occupied by Fe and X_2 occupied by Si, and (iii) both X_1 and X_2 occupied by Si. As X_1 and X_2 sites are equivalent, we do not expect significantly different relaxation behavior when we interchange Fe and Si on the $X_{1,2}$ sites. The results of the E_{inc} calculation as a function of the occupation of the X_1 and X_2 sites will be discussed later; here, we focus on the atomic relaxations around the U atom.

In a simple, qualitative picture, the origin of the atomic relaxations around an impurity can be attributed to two factors: (1) the size of the impurity as compared with the size of the host atoms and (2) the electrostatic forces acting on the atoms (nuclei). In our case, since the ionic radii of $U^{4+}$and Ca^{2+} are comparable,[31] when U substitutes Ca, we expect the relaxation behavior to be dominated by the electrostatics due to extra valence electrons.

In Table I, we list the relevant interatomic distances calculated with U located at the A site, along with the relative differences (in %) between these distances and those calculated for the undoped systems. Table I also contains the average U-O separations (four O's connected to the X sites, two O's connected to the X_1 site and two O's connected to X_2 site) as well as the U-$X_{1,2}$ distances. The negative values in Table I indicate inward relaxation (toward the U atom), while the positive values indicate outward relaxation (away from the U atom). The data listed in Table I show that the atoms surrounding U display qualitatively similar relaxation features regardless of the garnet composition.

First, we focus on the four O atoms, which connect U to the four X sites [not to X_1 and X_2, see Fig. 1(a)]. On average, these four O atoms display an inward relaxation for all garnet compositions. This is probably because the U^{4+} ion located at the A site generates a stronger Coulomb field than Ca^{2+}, and therefore, the surrounding O^{2-} anions experience a stronger attractive potential. The magnitude of the average inward relaxation of the four O's depends on the type of atom (Fe or Si) occupying X_1 and X_2. The relaxation is somewhat more pronounced when the X_1 and X_2 sites are occupied by different atomic species (Fe and Si). This is because if either X_1 or X_2 is occupied by Si, one of the two extra electrons introduced in the structure by U is accommodated by an Fe located further away, at one of the X sites. The oxidation state of this Fe changes from 3+ to 2+ and, consequently, it will exert a weaker Coulomb attraction on the surrounding O's. As a result, the O atom, which connects this Fe to U will move considerably closer to U, making the average distance between U and the four O's somewhat shorter. When both X_1 and X_2 are occupied by Si, the physical picture is quite different: since there are fewer Fe atoms in the vicinity of U, according to the calculations, only one of the extra electrons is transferred from U to an Fe atom. Therefore the attractive potential generated by U (3+ oxidation state) is weaker compared to the U^{4+} case. As a result, the average inward relaxation of the O's is less. (Table I only shows the average values, but some of the O's relax outward.)

TABLE II. Interatomic distances calculated when U is located at the *B* site in the garnet structure, along with the relative differences (in %) between these distances and those calculated for the undoped systems.

	Ti garnet		Zr garnet		Hf garnet		Sn garnet	
	distance (Å)	% change	distance (Å)	% change	distance (Å)	% change	distance (Å)	% change
U-O	2.16	8.00%	2.26	6.66%	2.26	7.95%	2.17	3.81%
U-X	3.58	3.03%	3.63	1.77%	3.62	1.91%	3.63	2.42%

An additional similarity in the relaxation pattern, characteristic to all garnets, is that the X_1 and X_2 sites relax outward, irrespective of the atomic species occupying them. This is most likely due to the combination of the size effect of the U atom and the increased Coulomb repulsion between the $U^{4+/3+}$ and the cations occupying X_1 and X_2.

The behavior of the O atoms, which connect U to the X_1 and X_2 sites, depends on the type of atom (Fe or Si) occupying X_1 and X_2. When both X_1 and X_2 are occupied by Fe, we observe an inward relaxation of these O atoms, regardless of the garnet composition. This relaxation behavior can be explained using the same argument as for the other O's: the U^{4+} ion creates a stronger attractive Coulomb field than the Ca^{2+} ion, therefore the O^{2-} anions will move closer to U. Furthermore, the inward relaxations of the two pairs of O's connected to the X_1 and X_2 sites are much more pronounced (range varies from 3.62% for Ti garnet to 6.72% for Zr garnet) as compared with the relaxations of the other four O's (from 0.56% for Sn garnet to 1.33% Zr garnet). This can be understood by considering the electron transfer that takes place from U to the neighboring Fe atoms, located at X_1 and X_2. Due to the charge transfer, the oxidation states will change from $Fe^{3+}$to Fe^{2+}, consequently, they will exert a weaker Coulomb attraction on the O atoms. This allows the two pairs of O atoms that are connected to the X_1 and X_2 sites to move closer to U as compared with the four O's that are connected to the other tetrahedral sites.

In the case when X_1 and X_2 are occupied by Fe and Si, respectively, the relaxation pattern of the O atoms is noticeably different. The two O's that connect U to its NN Fe (at X_1) relax strongly (by ∼6%) toward U, while the two O's that are connected to the X_2 site (occupied by Si) display outward relaxation (by ∼0.5%). The inward relaxation can be qualitatively explained using the same Coulomb potential-based argument. Conversely, the two O atoms located between U and the X_2 site, occupied by Si, only feel the attractive potential of U^{4+} and the repulsive effect due to U size (Si atoms do not accommodate extra electrons). The size effect being slightly stronger, the O's relax outward.

When both X_1 and X_2 are occupied by Si, we observe a 1–2% outward relaxation of the O's connected to X_1 and X_2. As previously discussed, when X_1 and X_2 are occupied by Si, U is in 3+ oxidation state; therefore it cannot generate a sufficiently strong attractive potential for the O's to overcome the repulsive effect due to its size.

2. Uranium at the B site

The octahedral site (*B* site) is shown in Fig. 1(b). The *B* site is coordinated by 6 O atoms and each O atom is connected to a tetrahedral site (*X* site), which can be occupied by Fe or Si. In Table II, we list the average U-O and U-*X* distances along with the percent change relative to interatomic distances of the undoped systems. When U^{4+} is located at the *B* site, no charge transfer is taking place, because it substitutes for a tetravalent cation (Ti, Zr, Hf, or Sn). Therefore we anticipate that the only effects regarding the relaxation are related to the larger ionic radius of U compared to the radii of cations it substitutes for.[31] The data in Table II confirm that the positive values of the percent difference indicate outward relaxation for all atoms surrounding U. In all garnet systems, the relaxation of the O atoms is much stronger (up to 8%) compared to the *X* sites (up to 3.03%). This makes sense because the O's are located much closer to U compared to the atoms at the *X* sites. We do not observe a consistent trend in the relaxation pattern around the *B* site as a function of *X* site occupation (Fe or Si).

B. Spin configuration

The U atom has more electrons outside a closed shell (the electronic configuration of the preceding noble gas) as compared with Ca, therefore, when placed at the *A* site in $Ca_3(Ti,Zr,Hf,Sn)_2(Fe_2Si)O_{12}$, it provides extra valence electrons to the system. These electrons can be accommodated by the Fe ions located in the vicinity of U. However, since the interatomic distances between U and Fe are sufficiently large, such that substantial orbital overlap is hindered, the precise mechanism of electron transfer is not straightforward. Instead of a direct coupling between the U *f* and Fe *d* shell, the charge transfer is more likely to occur through a mechanism similar to the double exchange interaction described by Zener.[32,33] Since the U and Fe ions are connected through closed shell O^{2-} ions, the electron transfer from U to Fe happens as a simultaneous transition of electrons from U to O^{2-} and from O^{2-} to Fe. Since these "transfer electrons" carry their own spins, the charge transfer is energetically more favorable if the electrons do not have to change their spin direction as they move from U to Fe (via the O). The Fe *d* shell being half filled, with all its unpaired electrons pointing in the same direction (Hund's rule), it can only accommodate electrons with spins oriented in the opposite direction. As a result, the transfer electrons will be able to keep their spin orientation as they travel from U to Fe, only if the spins of the U *f* shell and the Fe *d* shell are antiparallel. In other words, there is an antiferromagnetic (AFM) coupling of the U and Fe spins via the transfer electrons, which contributes to lowering the energy of the system and to increasing the stability of U in the garnet structure.

Because DFT is a single-particle theory, it obviously cannot describe this rather complex, many-body, double exchange

TABLE III. Total energy differences between the FM and AFM configurations of the U f and the surrounding Fe d shells. No convergent solution was obtained for the Ti-containing garnet, in FM configuration, with X_1 and X_2 occupied by Si. The values are given in meV.

	Ti garnet	Zr garnet	Hf garnet	Sn garnet
$X_1 = X_2 =$ Fe	40.21	11.34	40.66	83.45
$X_1 =$ Fe, $X_2 =$ Si	13.36	13.07	16.40	16.11
$X_1 = X_2 =$ Si	. . .	43.39	153.95	50.83

interaction. Nevertheless, the total energy calculations within DFT provide clear evidence that the AFM coupling of the U f and the NN Fe d spins is more stable than the ferromagnetic (FM) configuration. This is consistent with the charge transfer mechanism proposed. The total energies in both FM and AFM setups with U located at the A site have been calculated, and the energy differences listed in Table III. The AFM setup is energetically more favorable regardless of the garnet composition or the atomic configuration around U, confirming that the f-$d$coupling mechanism is a plausible explanation. Total energy calculations with U located at the B site were completed. In this case, the energy differences between the FM and AFM configurations are less than 10 meV/cell, regardless of the garnet composition.

C. Electronic structure of the U-containing systems

1. Uranium at the A site

In order to understand the electronic interaction of U with the host $Ca_3(Ti,Zr,Hf,Sn)_2(Fe_2Si)O_{12}$ garnet, electronic-structure calculations were completed in which U was treated as a substitutional impurity, located successively at the A and B sites.

In the case when U was placed at the A site, three different atomic configurations were used: both X_1 and X_2 occupied by Fe, X_1 and X_2 occupied by Fe and Si, respectively, and both X_1 and X_2 occupied by Si. In general, depending on the number of Fe atoms occupying the X_1 and X_2 sites, there were two types of electronic configurations: one in which two electrons are transferred from the U atom to two of the neighboring Fe atoms, resulting in a U^{4+} and two Fe^{2+} ions, and one in which only one electron is transferred, leaving U as 3+ and producing only one Fe^{2+} ion. The former occurs when there is at least one Fe atom located at X_1 or X_2, while the latter takes place when both X_1 and X_2 are occupied by Si. This is consistent with the idea that the more Fe atoms in the vicinity of U, the higher the probability for the electron transfer to occur.

In order to illustrate the two types of electronic configurations, we describe two particular cases, with electronic structures characteristic to the entire class: (i) for the U^{4+} case, $Ca_3Ti_2(Fe_2Si)O_{12}$ with X_1 and X_2 occupied by Fe, and (ii) for the U^{3+} case, the same $Ca_3Ti_2(Fe_2Si)O_{12}$ with X_1 and X_2 occupied by Si.

The calculated total and partial electronic density of states (DOS) of $Ca_3Ti_2(Fe_2Si)O_{12}$ with one U atom located at the dodecahedral site (A site), for the case when both X_1 and X_2 are occupied by Fe, are shown in Fig. 2. The two Fe atoms occupying X_1 and X_2 are labeled Fe_1 and Fe_2. In order to identify the changes in the electronic structure produced by the presence of U, the total DOS of the U-containing garnet was calculated, as shown in Fig. 2(a), for the total DOS of the pure $Ca_3Ti_2(Fe_2Si)O_{12}$ system.[14] The presence of the U atom at the A site, in addition to the small perturbations produced in the valence band (VB) and conduction band (CB), introduces several new features in the electronic structure of the system [indicated by arrows in Fig. 2(a)]: a sharp peak in the spin-up channel, at the bottom of the VB, at approximately 6 eV below the Fermi level (E_F), a defect state in the band gap, right at the E_F, and new electronic states in the CB, at approximately 4 eV above the E_F. To understand the parentage of these states, we calculated the partial DOS (PDOS) associated with the 5f orbital of U, the 3d orbitals of the $Fe_{1,2}$ atoms located at the $X_{1,2}$ sites, and the 2p orbitals of the four O atoms which connect U to Fe_1 and Fe_2. From the PDOS plots, shown in Figs. 2(b)–2(h), it is evident that the origin of the new features in the DOS has to be linked to the 5f orbitals of the U atom and to the 2p and 3d orbitals of the O and Fe atoms, respectively, located in the immediate vicinity of U.

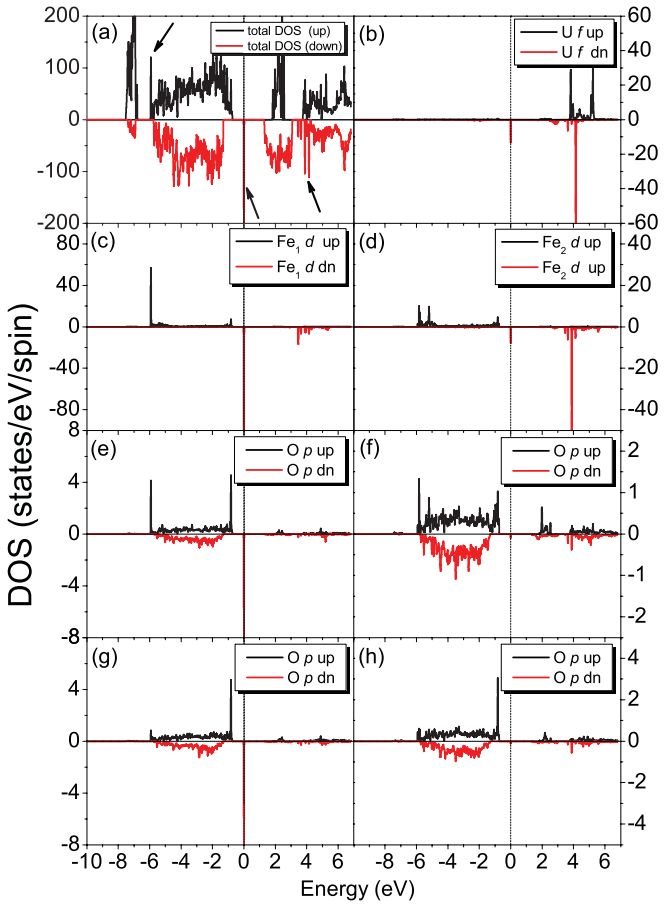

FIG. 2. (Color online) (a) The total DOS of $Ca_3Ti_2(Fe_2Si)O_{12}$ with one U atom located at the A site (substituting Ca), and the partial DOS associated with (b) the U f orbital, (c) and (d) the d orbitals of the Fe atoms occupying X_1 and X_2, (e)–(h) the p orbitals of the four O atoms connecting Fe_1 and Fe_2 to U. The arrows in (a) indicate the new features introduced by the presence of U at the A site, as compared to the DOS of the pure $Ca_3Ti_2(Fe_2Si)O_{12}$ system.

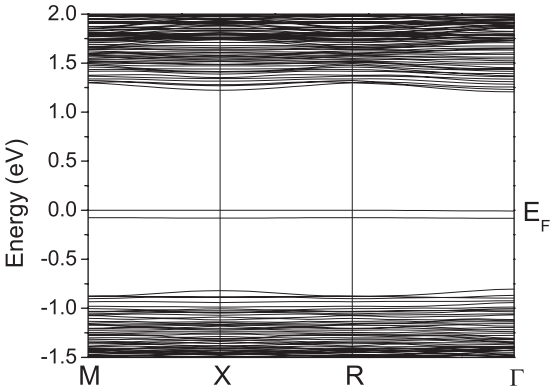

FIG. 3. The electronic band structure of $Ca_3Ti_2(Fe_2Si)O_{12}$ with one U atom located at the A site and Fe occupying both X_1 and X_2. The arrows indicate the new features in the electronic structure introduced by the presence of U at the A site. The two localized bands located near E_F are associated with the U f orbitals with contributions coming from the Fe atoms located at X_1 and X_2, and their NN O atoms.

The presence of U at the A site clearly perturbs the host VB and CB states and gives rise to new defect states. The extra two electrons introduced by U are transferred to the NN Fe_1 and Fe_2 atoms, changing their oxidation states from 3+ to 2+. As a result, the spin-down states in the d shells of both Fe_1 and Fe_2 become occupied and lowered in energy just below the E_F, within the band gap. Since these states are energetically almost degenerate, they show up in Fig. 2 as one state. However, on closer inspection of the calculated band structure, shown in Fig. 3, there are indeed two, nearly degenerate, and almost dispersionless states located in the vicinity of E_F. These electronic states also display a strong O p orbital character, since the charge transfer takes place via the O $p$orbitals, consistent with the double exchange mechanism. This is clearly visible in Figs. 2(c), 2(e), and 2(g), showing the PDOS associated with the d orbital of Fe_1 and p orbitals of two O atoms that connect Fe_1 to U, respectively. To further analyze the nature of these two states, Fig. 4 displays the charge density distribution in the energy range in which the corresponding states are located. These states are localized around the U, with contributions from the Fe atoms located at X_1 and X_2, and their NN O's.

Figures 2(c), 2(e), and 2(g) illustrate the strong hybridization between the Fe_1 d and the O p orbitals that develops in the spin-up channel of the VB due to the charge transfer process. This p-d mixing gives rise to the narrow peak at the bottom of the VB (indicated by the arrow), which is the bonding state between the Fe_1 3d and O 2p orbitals. The corresponding antibonding combination is located at the top of the VB. A similar physical picture is valid for Fe_2 and its NN O atoms [Figs. 2(d), 2(f), and 2(h)], although the degree p-d mixing is less pronounced. Figure 2(b) shows the PDOS associated with the U $f$orbitals. Since U is in 4+ valence state, it has 12 empty $f$orbitals (seven spin-up and five spin-down). These states are resonant in the CB and hybridize with other CB states (such as the empty Fe_1 and Fe_2 $d$states). The occupied U f orbitals are localized in the band gap and contribute to the defect state, together with a linear combination of $Fe_{1,2}$ $d$and O p orbitals.

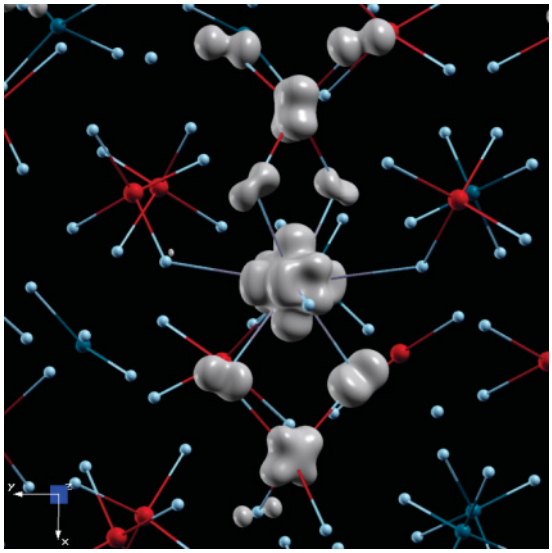

FIG. 4. (Color online) The charge density distribution calculated for the two defect bands shown in Fig. 3 that have eigenvalues close to E_F. The contribution to the charge density comes from the U 5f, Fe_1 and Fe_2 3d, and the O 2p orbitals.

When there are no Fe atoms in the immediate vicinity of U (i.e., both X_1 and X_2 sites are occupied by Si), only one of the two extra electrons introduced by U is transferred to an Fe atom located at one of the X sites [see Fig. 1(a)]. Although the charge transfer mechanism is similar to the previously described case, since only one electron is transferred, the resulting electronic structure is considerably different. In Fig. 5, we show the electronic band structure of $Ca_3Ti_2(Fe_2Si)O_{12}$ with one U atom located at the A site in an atomic configuration where X_1 and X_2 are occupied by Si. A major difference as compared with the previous case is that now, there are four defect bands located in the band gap, in the vicinity of E_F. They are highly localized, showing almost no dispersion at all. To identify the origin of these states, the charge density distribution within the energy range where the bands are located was plotted (see Fig. 6). The contributions to the defect states come from the U atom and one of the Fe atoms located at an X site. From the analysis of the d orbital occupation and the spin magnetic moment of this

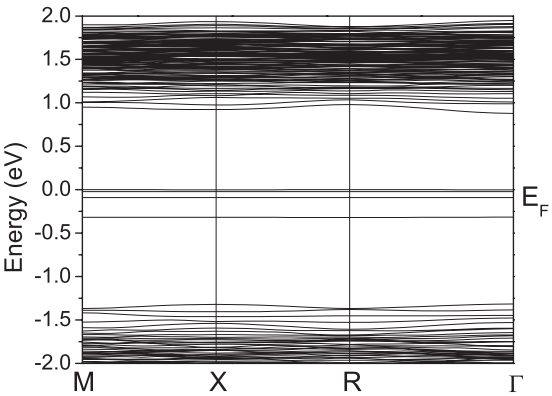

FIG. 5. The electronic band structure of $Ca_3Ti_2(Fe_2Si)O_{12}$ with one U atom located at the A site and Si located at both X_1 and X_2. There are four narrow bands in the vicinity of E_F.

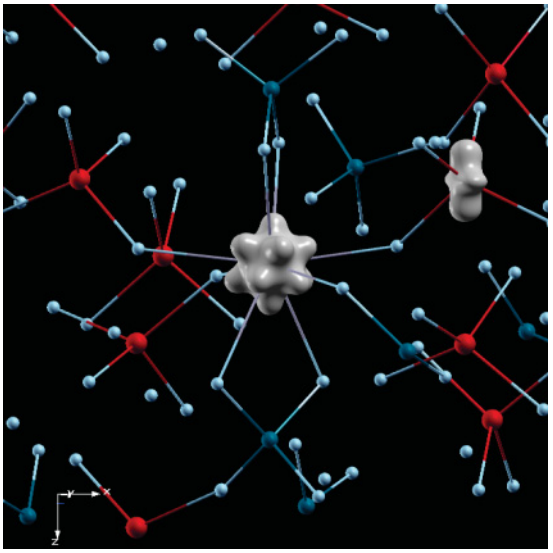

FIG. 6. (Color online) The charge density distribution associated with the four bands located near E_F, as shown in Fig. 5. The main contributions come from the *f* orbitals of U and *d* orbitals of one Fe.

Fe atom ($\mu_{\mathrm{Fe}} = 3.7\,\mu_B$ compared to $\sim 4.2\,\mu_B$ for the rest of the Fe atoms), we identify this Fe as the one that accommodates the extra electron introduced by U. The charge transfer to this Fe atom does not happen randomly: in all four garnet systems, the electron is always transferred to the Fe atom via the O atom located closest to U. This is consistent with the double exchange mechanism described in Sec. III B.

The origin of the four bands in the vicinity of E_F can be interpreted as follows. As a result of the charge transfer, the oxidation state of one Fe changes from 3+ to 2+, consequently an additional (spin-down) *d* state becomes occupied and lowered in energy just below the E_F. Uranium, being able to transfer only one of its two extra electrons to the neighboring Fe atom, becomes 3+ with 3 occupied *f* orbitals. The 3 U *f* orbitals, together with the Fe *d* orbital, contribute to the formation of the 4 electronic states in the band gap.

Despite the fact that the gap states do not show O *p* character, there is a strong O*p*-Fe *d* hybridization in the spin-up states, over the VB range. This mixing gives rise to bonding and antibonding states at the bottom and top of the VB, similar to the previous atomic case. The unoccupied U *f* states are located higher in the CB.

2. *Uranium at the B site*

When U is located at the octahedral site (*B* site), it replaces an atomic species in 4+ oxidation state (Ti, Zr, Hf, or Sn). Since U is also in 4+ state, no electron transfer is necessary in order to maintain the charge balance of the formula unit. Therefore there is no significant change in the electronic structure when U is at the *B* site.

Here, again, we only focus on one system [$Ca_3Zr_2(Fe_2Si)O_{12}$], since the electronic behavior of the other three systems is similar regarding the incorporation of U at the *B* site. Figures 7(a) and 7(b) show the total DOS of the U-doped $Ca_3Zr_2(Fe_2Si)O_{12}$ and the partial DOS associated with the U *f* states. The only significant difference as compared with the DOS of the pure $Ca_3Zr_2(Fe_2Si)O_{12}$ (see

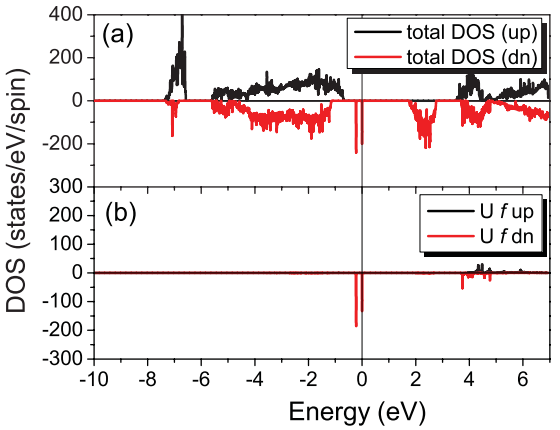

FIG. 7. (Color online) (a) The total DOS of $Ca_3Zr_2(Fe_2Si)O_{12}$ with one U located at the octahedral site (*B* site). The only significant difference compared to the DOS of the pure of $Ca_3Zr_2(Fe_2Si)O_{12}$ is related to the presence of the localized electronic states near E_F. (b) These states originate from the occupied *f* orbitals of U.

Ref. 14) is related to the presence of two narrow states in the band-gap region, just below E_F. These states originate from the U *f* states (U^{4+} has two occupied *f* orbitals), and they are strongly localized. The unoccupied U *f* states are located at higher energies, in the CB, as shown in Fig. 7(b).

D. Incorporation energies

Based on experimental results, the garnet structure can incorporate actinide ions. Furthermore, there is evidence that ferric garnets, in which the Si^{4+} ions at the tetrahedral sites are replaced by Fe^{3+}, have high isomorphic capacity with respect to actinides.[5,6] The enhanced actinide capacity has been related to the increase in the unit-cell volume when the smaller Si is replaced by a larger Fe.[31] In order to see whether the role of Fe in the incorporation mechanism is related exclusively to its size, the E_{inc} of U was calculated for a series of different atomic configurations in which the number of Fe atoms in the vicinity of U was varied, while holding the overall chemical composition constant. This minimizes the size effect, such that the E_{inc} mostly depends on the electronic interaction that takes place between U and the atoms located in its vicinity.

The method used for the calculations of the E_{inc} is similar to the one described in Ref. 14, with the difference that the atomic relaxations are calculated using Hubbard *U* parameters for the Fe *d* and U *f* states. The charge-balanced formula of the U-containing garnet, with U^{4+} at the *A* site, can be derived from the $Ca_3B_2(Fe_2^{3+}Si)O_{12}$, ($B$ = Ti, Zr, Hf, Sn), by substituting one Ca^{2+} ion with one U^{4+} and two Fe^{3+} ions with two Fe^{2+}. The incorporation energies of U^{4+} into the garnet structure were calculated according to the following reactions:

$$\mathrm{UO_2} + \mathrm{Fe_2SiO_4} + \left[\mathrm{Ca_{24}}B_{16}\left(\mathrm{Fe_2^{3+}Si}\right)_8\mathrm{O_{96}}\right] \rightarrow \\ \rightarrow \left[\left(\mathrm{Ca_{23}U^{4+}}\right)B_{16}\left(\mathrm{Fe_2^{2+}Fe_{14}^{3+}Si_8}\right)\mathrm{O_{96}}\right] + \mathrm{Fe_2O_3} + \mathrm{CaSiO_3}, \quad (1)$$

$$\mathrm{UO_2} + \mathrm{Fe_2SiO_4} + \mathrm{SiO_2} + \mathrm{Al_2O_3} + [\ldots] \rightarrow [\ldots] \\ + \mathrm{Fe_2O_3} + \mathrm{CaAl_2Si_2O_8}, \quad (2)$$

TABLE IV. Calculated incorporation energies of U at the *A* and *B* sites. The values are given in eV.

$Ca_3B_2(Fe_2Si)O_{12}$			B = Ti	B = Zr	B = Hf	B = Sn
U at *A* site	Eq. (1)	$X_1 = X_2 =$ Fe	−0.06	0.05	0.09	0.17
		$X_1 =$ Fe, $X_2 =$ Si	0.41	1.20	0.86	0.93
		$X_1 = X_2 =$ Si	2.40	1.30	1.43	1.85
	Eq. (2)	$X_1 = X_2 =$ Fe	−0.45	−0.34	−0.29	−0.22
		$X_1 =$ Fe, $X_2 =$ Si	0.02	0.81	0.47	0.54
		$X_1 = X_2 =$ Si	2.01	0.91	1.04	1.46
U at *B* site	Eq. (3)	...	0.83	1.45	0.66	0.61

where B stands for Ti, Zr, Hf, or Sn. In Eq. (2), square brackets represent the pure garnet (left-hand side) and the U-containing garnet (right-hand side). In all calculations, UO_2 is chosen as the source of U, while different mineral species are used as sources and sinks for Ca and Fe. The total energies of the source and sink minerals were calculated using the same computational parameters that were used for the garnet systems. As described in Sec. III C, when the X_1 and X_2 sites are occupied by Si, the oxidation state of U is 3+. The composition of the (U^{3+})-containing system can be obtained by substituting one Ca^{2+} ion with one U^{3+} and incorporating one Fe^{2+} at the X site previously occupied by a Fe^{3+} ion. The incorporation energies of U^{3+} have been calculated based on Eqs. (1) and (2), but on the right-hand side the (U^{4+})-containing system is replaced by $[(Ca_{23}U^{3+})B_{16}(Fe^{2+}Fe^{3+}_{15}Si_8)O_{96}]$.

In order to calculate the E_{inc} of U at the *B* site, we used an equation similar to Eqs. (1) and (2), with UO_2 as source for U and BO_2 (B = Ti, Zr, Hf, Sn) as sink for the element at the *B* site:

$$UO_2 + Ca_{24}B_{16}(Fe_2Si)_8O_{96} \rightarrow Ca_{24}(B_{15}U)(Fe_2Si)_8O_{96} + BO_2, \quad (3)$$

The calculated E_{inc} are listed in Table IV. First, by comparing the results obtained by Eqs. (1) and (2), we note that E_{inc} depends on the mineral species used in the calculations as sources and sinks for Ca and Fe. This observation is consistent with the results described in Ref. 14, that is the stability of U within the garnet structure can be related to the geological stability of minerals employed in the calculations. Second, and more importantly, the E_{inc} are highly sensitive to the number of Fe atoms located in the immediate vicinity of U, at the X_1 and X_2 sites. For both Eq. (1) and Eq. (2), the incorporation energies increase drastically when the number of Fe atoms occupying the X_1 and X_2 sites decreases. This is most evident in the case of the Ti-containing system, where the E_{inc} increases by 2.46 eV as the Fe atoms at $X_{1,2}$ are replaced by Si. Also, when X_1 and X_2 are occupied by Fe, all the E_{inc} calculated using Eq. (2) are negative, suggesting that in this atomic configuration, large amounts of U can be incorporated into the garnet structure.

From the analysis of the atomic relaxations around the U atom (see Sec. III A) with both X_1 and X_2 being occupied by Fe, the U-O distances decrease, indicating that the size of the dodecahedral site (*A* site) becomes smaller as compared with the case when X_1 and X_2 are occupied by Si (or Fe and Si). This is a clear indication that the stability of the garnet structure with U is primarily related to the electronic interactions between the U and Fe atoms, and the "size effect" of the Fe atom does not play a role in the incorporation mechanism of U into the structures of ferric garnets.

A further evidence in this direction comes from the fact that when X_1 and X_2 are occupied by Fe, the incorporation of U in the Ti garnet is always favored, even though, it has the smallest calculated lattice constants of all garnets under investigation.[14] The smaller structural parameters of the Ti garnet produce larger U-O-Fe orbital overlap and therefore the charge transfer, which stabilizes the U inside the structure, takes place with a higher probability. This physical picture is consistent throughout the Ti, Zr, Hf series: there is a direct correlation between the lattice parameters (a_{Ti} = 12.44 Å, a_{Zr} = 12.76 Å, and a_{Hf} = 12.71 Å) and the incorporation energies (see Table IV for $X_1 = X_2$ = Fe). From the data listed in Table IV, we notice that when both X_1 and X_2 are occupied by Si, the incorporation energies are inversely correlated with the lattice parameters. In this case, since only one electron is transferred from U to its neighbors, the electronic interactions do not play a significant role in the incorporation mechanism, and therefore the incorporation energies are mainly determined by the size of the structural sites.

When U is located at the octahedral site (*B* site), the calculated incorporation energies listed in Table IV are relatively high suggesting that the incorporation of large amounts of U at this site is improbable.

IV. CONCLUSIONS

Ab initio electronic structure calculations within the DFT were used to investigate the structural and electronic properties of U-containing $Ca_3(Ti,Zr,Hf,Sn)_2(Fe_2Si)O_{12}$ garnet. In order to deal with the localized U *f*and Fe *d* orbitals, we have explicitly taken into account the orbital-dependent Coulomb interaction by employing the GGA + U method.

When U is at the *A* site, substituting for Ca, the extra valence electrons introduced into the structure are accommodated by the Fe atoms in the vicinity of U. Since the U-Fe distances are quite large (more than ∼3.2 Å), there is no substantial *f*-*d* orbital overlap that could facilitate a direct U-Fe coupling. Therefore the charge transfer from U to Fe is more likely to happen through the nonmagnetic O ions (located between U and Fe) by a double exchange mechanism. This indirect coupling of the U and Fe spins through the "transfer-electrons" leads to the lowering of the energy of the structure when the spins of the *f* and *d*shells are antiparallel.

The atomic relaxation around the U atom can be qualitatively described by considering the subtle balance between the size effect of the large U atom and the electrostatic interactions due to the extra electrons introduced by U. A universal relaxation feature, characteristic to all four garnet systems, is that the O atoms that connect U to the Fe ions, which accommodate the extra electrons, always relax toward the U. This is because the Coulomb field of the U^{4+} ion is stronger than that of Ca^{2+}, and at the same time, the strength of the Coulomb attraction between the O^{2-} and the Fe ions, which accept extra electrons, decreases. These two effects combined overcome the size effect of U and make the O to relax toward U, away from Fe. The relaxation of the atoms, which are not involved in the charge transfer, is generally dominated by the size effect of U, thus they relax away from U. This is especially the case when U is located at the *B* site, and no charge transfer occurs.

The presence of U at the *A* site perturbs the VB and CB of the garnet and gives rise to new electronic states located in the band-gap region. The extra electrons are accommodated by Fe; therefore some spin-down *d* states become occupied and lowered in energy below the E_F. Since the charge transfer takes place via the O atoms, there is a strong O *p*-Fe *d* hybridization throughout the VB.

When U^{4+} is at the *B* site, it substitutes for an atomic species in the same oxidation state, therefore no charge transfer is necessary to maintain the charge balance. In this case, the presence of U induces only small changes in the electronic properties of the system.

The incorporation energy of U into the garnet structure depends significantly on the number of Fe atoms occupying the *X* sites. There is a dramatic increase in E_{inc} as the number of Fe atoms in the vicinity of U decreases. This indicates that the interactions at the electronic level, which take place between U *f* and Fe *d* states, play a crucial role in the stability of U inside the garnet structure. The atomic relaxations indicate that the size of the dodecahedral site (*A* site) decreases when both X_1 and X_2 are occupied by Fe. This suggests that the larger size of Fe as compared with Si, does not play a role in the increased actinide capacity of the ferric garnet.

The negative incorporation energies (Table IV) indicate that garnets with Fe^{3+} cations occupying the tetrahedrally coordinated sites are promising materials for incorporation and immobilization of uranium and, possibly, other actinides (Pu, Np). The incorporation mechanism described here is quite general and applicable to a large class of elements with partially filled, localized orbitals [such as transition metals (TM) or rare earths (RE)]. Even though the results presented in this paper are, to some extent, semiquantitative, the work is important to understand the mechanism of incorporation of U in garnet matrices and to enhance our understanding of actinide materials.

ACKNOWLEDGMENTS

This work was supported as part of the Materials Science of Actinides, an Energy Frontier Research Center, funded by the Office of Basic Energy Sciences under Award No. DE-SC0001089.

*rakzsolt@umich.edu

[1] R. C. Ewing, Proc. Natl. Acad. Sci. USA **96**, 3432 (1999).
[2] R. C. Ewing, W. J. Weber, and J. Lian, J. Appl. Phys. **95**, 5949 (2004).
[3] R. C. Ewing, Earth Planet Sc. Lett. **229**, 165 (2005).
[4] B. E. Burakov, E. B. Anderson, D. A. Knecht, M. A. Zamoryanskaya, E. E. Strykanova, M. A. Yagovkina, D. Wronkiewicz, and J. Lee, in *Scientific Basis for Nuclear Waste Management XXII*, edited by D. J. Wronkiewicz and J. H. Lee, Proceedings of the Materials Research Society, Vol. 556, p. 55, (1999).
[5] S. V. Yudintsev, A. A. Osherova, A. V. Dubinin, A. V. Zotov, and S. V. Stefanovsky, in *Scientific Basis for Nuclear Waste Management XXVIII*, edited by J. M. Hanchar, S. Stroes-Gascoyne, and L. Browning, Proceedings of the Materials Research Society, Vol. 824, p. 287 (2004).
[6] T. S. Youdintseva, Geol. Ore Deposit+ **47**, 403 (2005).
[7] N. P. Laverov, S. V. Yudintsev, T. S. Yudintseva, S. V. Stefanovsky, R. C. Ewing, J. Lian, S. Utsunomiya, and L. M. Wang, Geol. Ore Deposit+ **45**, 423 (2003).
[8] S. Utsunomiya, S. Yudintsev, and R. C. Ewing, J. Nucl. Mater. **336**, 251 (2005).
[9] T. S. Livshits and S. T. Yudintsev, in Proceedings in the 1st European Chemistry Congress, Budapest p. 399 (2006).
[10] T. S. Livshits, A. A. Lizin, J. M. Zhang, and R. C. Ewing, Geol. Ore Deposit+ **52**, 267 (2010).
[11] K. R. Whittle, M. G. Blackford, G. R. Lumpkin, K. L. Smith, and N. J. Zaluzec, in *Scientific Basis for Nuclear Waste Management XXXII*, edited by R. B. Rebak, N. C. Hyatt, and D. A. Pickett, Proceedings of the Materials Research Society, Vol. 1124, p. 1124-Q10-08 (2009).
[12] T. S. Livshits, Geol. Ore Deposit+ **50**, 470 (2008).
[13] B. I. Omel'yanenko, T. S. Livshits, S. V. Yudintsev, and B. S. Nikonov, Geol. Ore Deposit+ **49**, 173 (2007).
[14] Zs. Rak, R. C. Ewing, and U. Becker, Phys. Rev. B **83**, 155123 (2011).
[15] I. O. Galuskina, E. V. Galuskin, T. Armbruster, B. Lazic, J. Kusz, P. Dzierzanowski, V. M. Gazeev, N. N. Pertsev, K. Prusik, A. E. Zadov, A. Winiarski, R. Wrzalik, and A. G. Gurbanov, Am. Mineral. **95**, 1172 (2010).
[16] P. E. Blochl, Phys. Rev. B **50**, 17953 (1994).
[17] G. Kresse and D. Joubert, Phys. Rev. B **59**, 1758 (1999).
[18] P. Hohenberg and W. Kohn, Phys. Rev. B **136**, B864 (1964).
[19] W. Kohn and L. J. Sham, Phys. Rev. **140**, 1133 (1965).
[20] G. Kresse and J. Furthmuller, Phys. Rev. B **54**, 11169 (1996).
[21] G. Kresse and J. Furthmuller, Comput. Mater. Sci. **6**, 15 (1996).
[22] G. Kresse and J. Hafner, Phys. Rev. B **47**, 558 (1993).
[23] G. Kresse and J. Hafner, Phys. Rev. B **49**, 14251 (1994).

[24]J. P. Perdew, K. Burke, and M. Ernzerhof, Phys. Rev. Lett. **77**, 3865 (1996).
[25]V. I. Anisimov, J. Zaanen, and O. K. Andersen, Phys. Rev. B **44**, 943 (1991).
[26]A. I. Liechtenstein, V. I. Anisimov, and J. Zaanen, Phys. Rev. B **52**, R5467 (1995).
[27]V. I. Anisimov and O. Gunnarsson, Phys. Rev. B **43**, 7570 (1991).
[28]V. I. Anisimov, I. S. Elfimov, N. Hamada, and K. Terakura, Phys. Rev. B **54**, 4387 (1996).
[29]Y. Baer and J. Schoenes, Solid State Commun. **33**, 885 (1980).
[30]H. Eschrig, M. Richter, and I. Opahle, *Relativistic Solid State Calculations, in Relativistic Electronic Structure Theory, Part II: Applications* (Elsevier, Amsterdam, 2004), pp. 723–776.
[31]R. D. Shannon, Acta Crystallogr. Sect. A **32**, 751 (1976).
[32]C. Zener, Phys. Rev. **81**, 440 (1951).
[33]C. Zener, Phys. Rev. **82**, 403 (1951).